Optical scanner system for high resolution measurement of lubricant distributions on metal strips based on laser induced fluorescence

Philipp Holz*[a], Christian Lutz[a], Albrecht Brandenburg[a]

Fraunhofer Institute for Physical Measurement Techniques IPM;
Heidenhofstrasse 8, 79110 Freiburg, Germany

ABSTRACT

We present a new optical setup, which uses scanning mirrors in combination with laser induced fluorescence to monitor the spatial distribution of lubricant on metal sheets.

Current trends in metal processing industry require forming procedures with increasing deformations. Thus a well-defined amount of lubricant is necessary to prevent the material from rupture, to reduce the wearing of the manufacturing tool as well as to prevent problems in post-deforming procedures. Therefore spatial resolved analysis of the thickness of lubricant layers is required. Current systems capture the lubricant distribution by moving sensor heads over the object along a linear axis. However the spatial resolution of these systems is insufficient at high strip speeds, e.g. at press plants.

The presented technology uses fast rotating scanner mirrors to deflect a laser beam on the surface. This 405 nm laser light excites the autofluorescence of the investigated lubricants. A coaxial optic collects the fluorescence signal which is then spectrally filtered and recorded using a photomultiplier. From the acquired signal a two dimensional image is reconstructed in real time. This paper presents the sensor setup as well as its characterization. For the calibration of the system reference targets were prepared using an ink jet printer.

The presented technology for the first time allows a spatial resolution in the millimetre range at production speed. The presented test system analyses an area of 300 x 300 mm² at a spatial resolution of 1.1 mm in less than 20 seconds. Despite this high speed of the measurement the limit of detection of the system described in this paper is better than 0.05 g/m² for the certified lubricant BAM K-009.

Keywords: laser induced fluorescence, lubricant distribution, laser scanner, autofluorescence, oil-film thickness, fluorescence imaging

1. INTRODUCTION

Current trends in metal processing industry require forming procedures which allow the production of components with extreme aspect ratios and acute edges. For these processes on one hand an increased amount of lubricants guarantee a long lifetime of the manufacturing tools and prevent the metal strips from rupture during metal forming. In contrast an increased amount of lubricants causes problems in post-deforming procedures such as welding or coating. Therefore current spray systems can dose lubricants in a spatial resolution of 100 mm. To monitor the spatial distribution of the lubricant thickness new measurement technology is required.

In industrial applications optical thickness measurements of lubricant layers are mainly realized by two different spectroscopic approaches. The first approach is the analysis of the light absorbed in the infrared spectral range by lubricants.[1] Existing systems based on IR-spectroscpy[1,2] use a sensor head which is mounted on a traversing unit to record the lubricant distribution on metal strips. Since closed oil layers are required for absorption measurements additional homogenization rolls are required to flatten oil droplets[1,2]. Due to the limited traversing speed of up to 1 m/s orthogonal to the movement of the metal strips these systems cannot analyze the complete metal surface at high strip speeds. At strip speeds of 2 m/s at press plants the distance between two measurement points in feed direction is up to 8 meters. For this reason systems mounted on traversing units are not capable of measuring the lubricant distribution in feed direction of metal strips.

*philipp.holz@ipm.fraunhofer.de; phone +49 761 8857-380; fax +49 761 8857-224; ipm.fraunhofer.de

The second approach to measure the thickness of lubricant layers in industrial applications is the use of laser induced fluorescence. Current sensors[3,2] which use this method in industrial applications use a sensor head, which is mounted on a traversing unit as well. Alternatively fluorescence images are captured with a camera, where for example the oil-film thicknesses in a piston-ring area has been measured.[4,5] The field of view of this setups are only of some square millimeters and dyes have to be used to enhance the fluorescence signals. Laser scanning can be used to overcome this limitation. A combined setup with scanning mirrors and laser induced fluorescence is described for systems used to monitor oil spills on the sea surface.[6,7] These systems are installed at airplanes. Components used in these setups are fairly expensive and not suitable for industrial applications.

Aim of the research leading to this paper was to develop a measurement system that meets the requirements on spatial resolution, speed and sensitivity to monitor and optimize the described industrial forming processes.

2. EXPERIMENTAL

To meet the described requirements on spatial resolution and film thickness sensitivity the developed system uses scanning mirrors in combination with laser induced fluorescence in order to monitor the spatial distribution of lubricants. For the characterization of the developed system custom designed samples are used.

2.1 Sensor design

The presented optical system is shown in figure 1. To ensure laser safety the optical setup is installed on top of a sample chamber. To achieve a good limit of detection we use a 405 nm diode laser module with 300 mW optical power for the excitation of the samples. The light of the laser is focused on the bottom of the sample chamber. To ensure laser safety the filter glass of the housing prevents the excitation laser from leaving the sample chamber. Further a low-power pointing laser at 635 nm is used to visualize the laser position during experiments. As shown in figure 1b both laser beams are aligned to the center of the scanning mirrors with several adjustment mirrors.

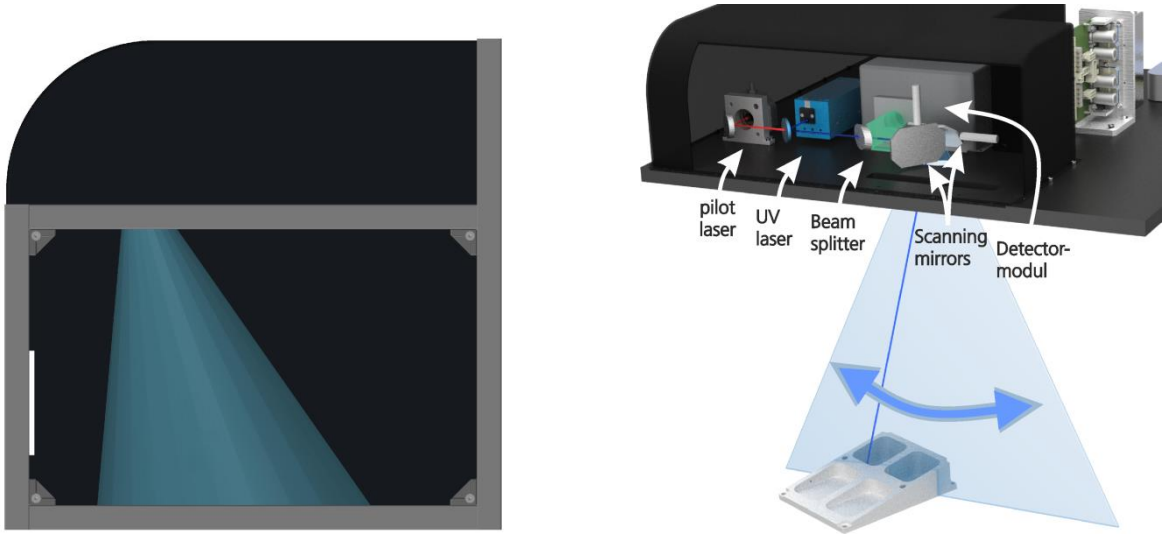

a) b)

Figure 1: Concept of the presented system. As shown in figure (a) the optical setup is installed on top of a sample chamber. Details on the optical setup are shown in the top view in figure (b).

During the scan the excitation laser induces fluorescence locally on the probe inside the sample chamber. A part of the fluorescence light is collected back by the scanning mirrors. A chromatic beam splitter is used to deflect fluorescence light in a wavelength range 420 to 520 nm on the detector. For the detection of the fluorescence signals we use a photomultiplier module.

In the presented setup we use a PC equipped with a PCI Express I/O card for data acquisition. The I/O card acquires the signal of the photomultiplier. In addition the I/O card provides the control voltages to positon the scanning mirrors as well as the control voltage for the amplification of the photomultiplier module. In addition to allow the selection of the sample, an integrated webcam captures the inside of the sample chamber. USB signals from the webcam and the laser module are converted to gigabit Ethernet signals inside the sensors housing to avoid electrical interferences at production environments.

Both scanning mirrors allow the deflection of the laser beams of an angle of $\alpha_{\max} = \beta_{\max} = \pm 20°$. As the optical system is installed 300 mm above the bottom of the sample chamber the field of view of the presented system is 300 x 300 mm². The scanning speed of the presented system is limited by the mechanical inertia of the utilized mirrors. The maximum mirror speed of the fast scanning direction was determined in experiments and is $v_{\max \alpha} = 4400\ °/s$. The maximum line frequency at full scanning angle is determined in experiments on $f_{\max \alpha} = 50$ Hz. At a sampling rate of 2.5 lines per millimeter the presented system needs less 20 seconds to analyze the complete field of view. The spatial resolution at this sampling rate was determined on 1.1 mm.

2.2 Image acquisition

The software of the presented system allows the flexible selection of the area to be scanned as well as the resolution r_{mm} in samples per mm to be acquired. To speed up the overall scanning process, a minimum angular range is computed for both scanner mirrors, which fully covers the selected planar region on the bottom of the sample chamber. To acquire an undistorted rectangular projection of the sample we calculate the corresponding scanning angles (α, β) for each position (x, y) on the base plate as follows:

$$\beta(y) = \tan^{-1}\left(\frac{y}{h_0}\right), \tag{1}$$

$$\alpha(x, y) = \tan^{-1}\left(\frac{x}{h(y)}\right) \quad \text{with} \quad h(y) = \sqrt{h_0^2 + y^2} + \delta_{\text{mirrors}} \tag{2}$$

The steps of the slow scanning axis β are adapted during the scan to directly match the rows of the undistorted image with the desired planar resolution. Due to a fixed sample rate f_{sample} in samples per seconds of the I/O card during the complete scan, the sampling positions do not exactly correspond to the pixel positions in each row. Thus, the pixel values need to be linearly interpolated between two neighboring samples. The sample rate is chosen to accord with the lateral image resolution assuming the maximum angular velocity $v_{\max \alpha}$ of the fast scanning axis. Hence, on average, the raw scan data is oversampled compared to the undistorted image.

The response of the movement of the scanning mirrors to the control signal varies depending on the selected area to be scanned. To determine the relation between sample number t and mirror position $\alpha(t)$ a reference scan is made at the beginning of each measurement.

2.3 Reference targets for sensor characterization

Stability of the presented system was characterized using a target made of Spectralon® fluorescence material (Labsphere Type 461: USFS-461-020; 2"). This fluorescence standard has the shape of a disc with a diameter of 2 inches. According to Labsphere the fluoropolymer material Spectralon® is used as a matrix for inorganic fluorophores which are photochemically stable when compared to their organic counterparts.[8] Figure 2 displays the fluorescence image of the reference target, which is used in this paper. To monitor the sensor stability, the average signal intensity of each fluorescence image, of the reference target, is monitored over several hours.

The spatial resolution of the presented system was determined by covering the reference target with a custom made etched aluminium stencil. The stencil consists of orthogonal placed windows at a width from 0.2 mm to 1 mm. An optical microscope was used to verify width and the distance of the etched windows. The fluorescence images of the sample target which is covered by the aluminium stencil are acquired by the presented system. The signal contrast between non-fluorescent areas covered by the stencil and fluorescent areas of the reference target is calculated to determine the spatial resolution. Values for the spatial resolution given in this paper refer to a signal contrast of 1:2. The

special resolution is defined as the period of the fluorescent areas, which is equivalent to two times the width of the etched windows.

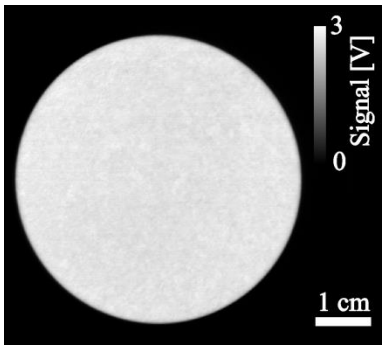

Figure 2: Fluorescence image of the reference target used in this paper. The image was acquired with the system presented in this paper.

2.4 Linearization of detector response

A wide dynamic range of fluorescence intensities can be detected by adjusting the amplification of the photomultiplier module. A linearization of the complete dynamic range can be achieved by calibrating the detector signals to a well-known stable light source. In this paper we use the installed laser as light source, since one goal of the work leading to this paper is to develop easy routines for the calibration of fluorescence measurement systems. As shown in equation 6 the fluorescence signal is proportional to the laser intensity I_0 if quantum yield Φ and absorbance αd are constant. Therefore the reference target described in section 2.3 is illuminated at a wide dynamic range I_0 to acquire the data for linearization. To achieve this wide dynamic range for illumination, different neutral density filters are installed in front of the laser. Following this procedure the laser power could be varied between $P_{0\,\mathrm{min}} = 8\ \mu\mathrm{W}$ to $P_{0\,\mathrm{max}} = 21\ \mathrm{mW}$. The laser power is changed periodically at all amplification settings to get reliable data of the photomultiplier response.

2.5 Calibration for quantitative measurements

The dependence of the fluorescence signal on film thicknesses is well described in literature[9]. According to Beer–Lambert law incident light with the intensity I_0 is attenuated proportional to the thickness d of an absorbing layer and the attenuation coefficient α of the medium at the wavelength λ_{ex} of the incident light. The intensity of the absorbed light $I_\mathrm{a}\,(\lambda_{ex})$ is

$$I_\mathrm{a}\,(\lambda_{ex}) = I_0\big(1 - e^{-\alpha(\lambda_{ex})d}\big). \tag{3}$$

For simplicity in this paper we use the attenuation coefficient α based on the natural logarithm, whereas in literature often the decadic attenuation coefficient is used.[9] The quantum yield ϕ is defined as the ratio of the number of emitted photons to the number of absorbed photons. The steady-state fluorescence intensity per absorbed photon can be expressed as a function of the wavelength of the emitted photons $F_\lambda(\lambda_{em})$ in nm^{-1}:

$$\int_0^\infty F_\lambda(\lambda_{em})d\lambda = \phi. \tag{4}$$

$F_\lambda(\lambda_{em})$ represents the fluorescence spectrum. In practice, the steady-state fluorescence intensity $I_f(\lambda_{em})$ measured at wavelength λ_{em} (selected by a monochromator with a certain wavelength bandpass $\Delta\lambda_{em}$) is proportional to $F_\lambda(\lambda_{em})$ and to the number of photons absorbed at the excitation wave length λ_{ex}.[9] Using equation 3 the fluorescence intensity can thus be written as

$$I_\mathrm{f}\,(\lambda_{ex},\lambda_{em}) = F_\lambda(\lambda_{em})\,I_0\big(1 - e^{-\alpha(\lambda_{ex})d}\big). \tag{5}$$

For low absorbance values αd the first term of the Taylor series of Equation 5 can be used:

$$I_\mathrm{f}\,(\lambda_{ex},\lambda_{em}) \approx F_\lambda(\lambda_{em})\,I_0\alpha(\lambda_{ex})d. \tag{6}$$

This relation shows that the fluorescence intensity is proportional to the film thickness d only for low absorbance values αd. Table 1 shows the deviation of the approximation with increasing absorbance.

Table 1: Deviation from linearity in the relation between fluorescence intensity and film thickness for various absorbance values αd

Absorbance αd	Deviation (%)
10^{-3}	0.1
10^{-2}	0.5
0.1	5.1
0.2	10.3

In practice fluorescence intensity which reaches the detector aperture depends on a on the sensor geometry, the properties of the optical components and the distance l between fluorescence emission and detector aperture. The spectral response of the detector further influences the detector signal U_d. These system-specific properties can be described in a proportional factor k

$$U_{\mathrm{d}}(\lambda_{ex}, \lambda_{em}) \approx k(\lambda_{em}) \frac{1}{l^2} I_{\mathrm{f}}(\lambda_{ex}, \lambda_{em}) \tag{7}$$

2.6 Samples for quantitative measurements

Samples with a known layer of lubricants are required to calibrate the system for quantitative measurements. We use the certified reference material BAM-K009 for the calibration of the system to ensure the repeatability of the experiments over a long period. BAM-K009 is a lubricant oil based on the additive free lubricant oil HVI 50 provided by Shell Global Solutions GmbH. Homogeneity and stability of the mass fraction of the boiling range C10 - C40 are certified by BAM Federal Institute for Materials Research and Testing.[10]

The optical properties of the lubricant oil BAM-K009 were characterized. A double-beam absorption spectrometer (Perkin Elmer, Lambda 900) was used to obtain the attenuation coefficient α(λ). The fluorescence spectrum $F_\lambda(\lambda)$ was obtain using a fluorescence spectrometer (Jasco, FP-8500). For both measurements 10 x 10 mm² quartz glass cuvettes were used.

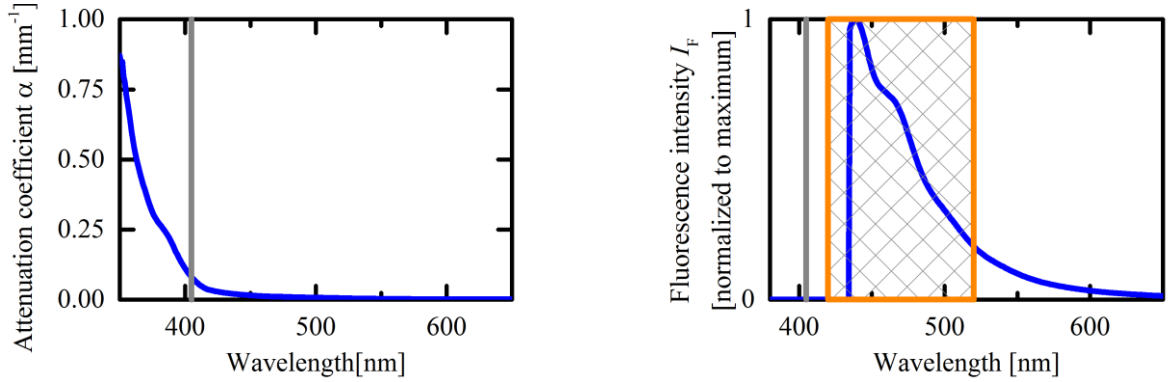

Figure 3: Attenuation coefficient (a) and fluorescence (b) spectrum of the certified lubricant oil BAM-K009. The attenuation coefficient α shown in (a) is based on the natural logarithm. In both figures the vertical line marks the wavelength of the 405 nm excitation laser used in this paper. The highlighted region in the fluorescence spectrum (b) marks the wavelength region which is detected by the system presented in this paper.

The vertical line shown in Figure 3 marks the wavelength of the 405 nm excitation laser used in this paper. The highlighted region in the fluorescence spectrum (b) marks the wavelength region which is detected by the system presented in this paper. The attenuation coefficient α shown in (a) is based on the natural logarithm, whereas in literature often the decadic attenuation coefficient is used.[9] As show in Figure 3 the attenuation coefficient of the lubricant oil BAM-K009 at 405 nm is $\alpha(405\ \mathrm{nm}) = 0.1\ \mathrm{mm}^{-1}$. In industrial applications the area density of lubricants is typically in the order of 1 g/m². Assuming a density of the lubricants of 900 kg/m³ the thickness of typical lubricant layers is in the

order of $d = 1.1$ µm. Based on this values the absorbance is $\alpha d = 10^{-4}$. Thus the deviation due to linear approximation shown in equation 5 is negligible.

For sample preparation different surfeces are coated with lubricant films using an ink jet printer (Fujifilm, Dimatix 2831). A high range of area densities can be achieved by varying the number of oil droplets per area. Figure 4 shows images of oil droplets on different surfaces.

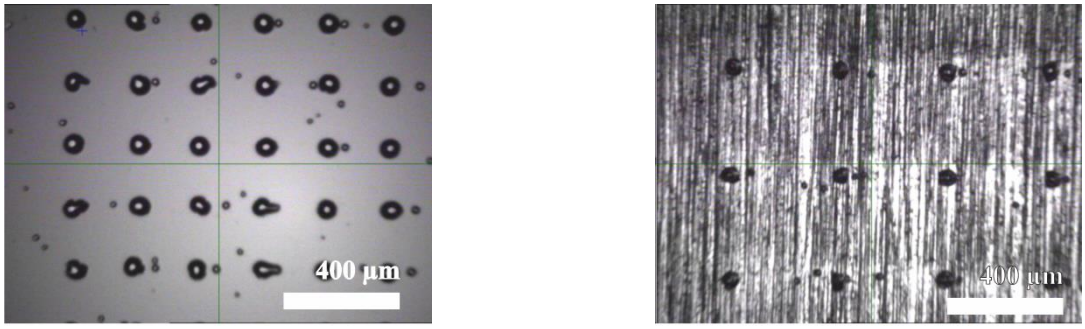

a) b)

Figure 4: To create different area densities single lubricant-droplets were printed using an ink jet printer on silicon (a) and aluminium (b) surfaces.

To determine the area densities the mass of a single was determined. Therefore the ink jet printer filled 7 x 10^6 droplets into a flask witch than was weighted using an analytical balance (Sartorius, CP225D). This experiment was repeated for seven times. The average mass of a single lubricant droplet based on all seven experiments is $m_{\mathrm{d}} = 8.5 \pm 0.4$ ng. Using this result the are density $\rho_A$of the lubricant is directly calculated from the number of droplets N per area A

$$\rho_A = \frac{N}{A} m_d \qquad (8)$$

For the results shown in this paper the distance between the lubricant droplets was varied in the range of 185 µm to 410 µm. Since the printed area is $A = 20 \text{ x } 20 \text{ mm}^2$ the number of droplets N varies in the range of 11 815 to 2 380. This leads to lubricant densities in the range of $\rho_A = 25.1 \pm 1.2$ µg/cm² to $\rho_A = 5.1 \pm 0.2$ µg/cm².

3. RESULTS

3.1 Sensor Repeatability

Repeatability is one of the most basic criteria of a system for use in quantitative measurements. After a warmup time of the sensor of 60 minutes the reference target was measured for 5 500 times over a period of over 55 hours. The result of the repeated measurement of the reference target is shown in Figure 5. The result of this experiment demonstrates good repeatability as the deviation of detected fluorescence signals is less than $\pm$ 2 % of the average fluorescence signal.

As shown in equation 5 the fluorescence signal is proportional to the laser intensity I_0 if quantum yield Φ and absorbance αd are constant. Thus the result shown in Figure 5 represents the combined deviation of all system components. Main sources of these deviations are deviations in laser power, detector response and analog digital conversion.

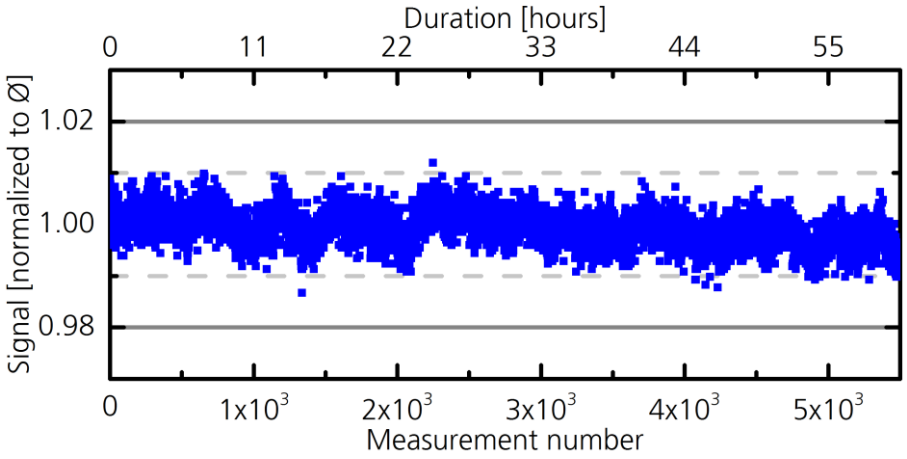

Figure 5: Repeatability of the presented system over 55 hours (5500 measurements). The Repeatability was analysed by repeated measurements of the reference target.

3.2 Spatial resolution

The spatial resolution describes the capability of an imaging system to distinguish between two signals emitted in close neighborhood. The result of the measurement of the reference target covered by the etched aluminium stencil is shown in Figure 6. The fluorescence image shown in Figure 6 was acquired at a sampling rate of $r_{mm} = 15$ px/mm. The reference target was placed in the center of the sample chamber.

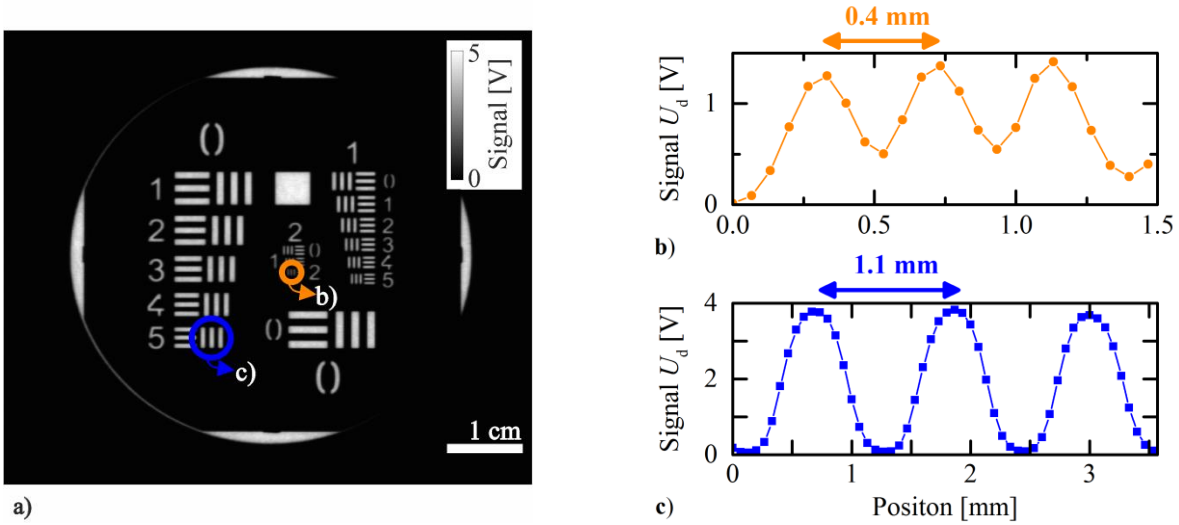

Figure 6: Fluorescence image (a) of the reference target covered with an etched aluminium stencil. The image was acquired at a sampling rate of $r_{mm} = 15$ px/mm with the presented setup. Intensity profiles for a period of the fluorescent areas of 400 µm (b) and 1.1 mm (c) are shown.

As shown in Figure 6b a factor two in intensity contrast between fluorescent and non-fluorescent areas is achieved at periods down to 400 µm with the system presented in this paper. This means that gaps between lubricant droplets down to a width of 200 µm can still be visualized.

3.3 Linearization of detector response

Linearity of the detector response is another basic requirement for systems for use in quantitative measurements. As described in section 2.4 we use the Labsphere reference target to analyze the detector response. We achieved a high

dynamic range of fluorescence signals at the detector by installing different neutral density filters in the path of the excitation laser. Figure 7 shows the detector response for a variation of signal intensity over six orders of magnitudes.

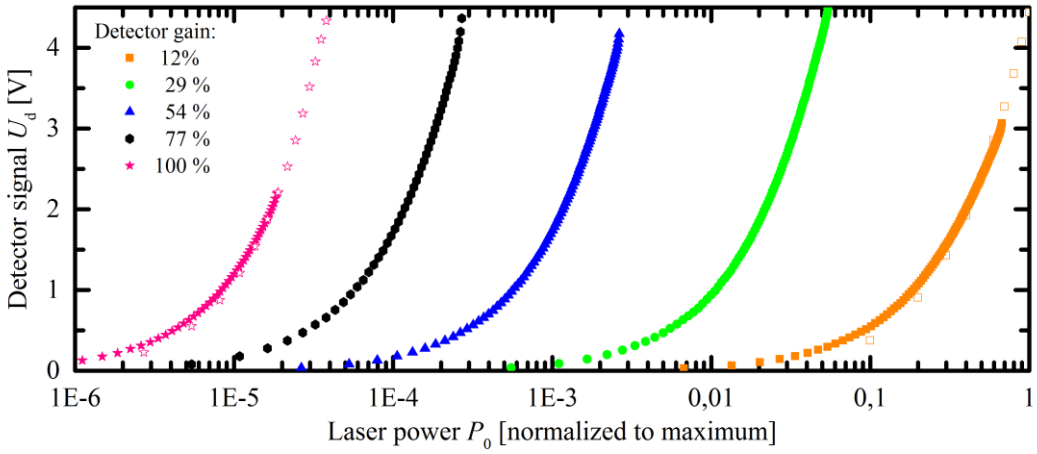

Figure 7: Detector response to fluorescence signal intensities over a range of six orders of magnitudes. This high dynamic range of fluorescence signals at the detector was achieved by installing different neutral density filters in the path of the excitation laser.

As shown in Figure 7 five gain settings of the photomultiplier module are sufficient to enable the presented system to detect fluorescence signal intensities over a range of six orders of magnitudes. The gain settings are stored in the software of the presented systems. Before starting a scan the user has to select a suitable amplification setting. As shown in the figure the amplification settings overlap. The overlap ensures a good use of the liner range of the detector for arbitrary fluorescence intensities. A more detailed view on the detector response for the amplification settings 12 % and 100 % is shown in Figure 8.

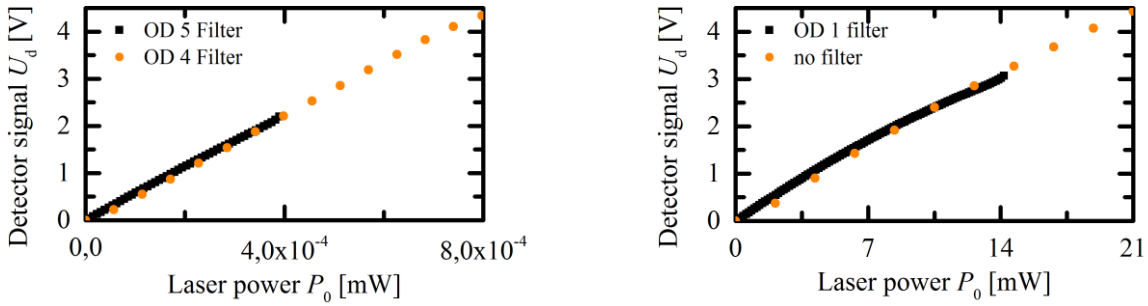

a) b)

Figure 8: Detector response to fluorescence signal for the amplification settings 100 % (a) and 12 % (b). The figures show the linearity of the response at each amplification setting.

Figure 8 shows a good linear response of the detector signal at the amplification settings 100 % (a) and 12 % (b). Both graphs compare measurements using two types of neutral density filters. Detector signals for hundred laser power settings were recorded for each neutral density filter installed.

3.4 Calibration for quantitative measurements

The results presented in section 3.1 to 3.3 are prerequisites for quantitative measurements. The result shown in Figure 9 illustrates the feasibility for quantitative measurements of the thickness of lubricant layers. Figure 9b shows a fluorescence image of a silicon wafer that was coated using an ink jet printer as described in section 2.6.

Figure 9a clearly shows the increase of the fluorescence signal at increasing densities of lubricant droplets per area. The bright spots in the fluorescence image are dust particles. For the analysis the average signal intensity of each area is calculated. The plot in Figure 9a shows the relation between this average intensities and the area density of lubricant

based on the number of printed lubricant droplets. The dashed line in Figure 9a clearly visualizes the linear relation between the fluorescence signal and the thickness of the lubricant layer, as expected in equation 6. The error bars shown in Figure 9a occur from the measured repeatability of ±2 % and the weight uncertainty of the average drop mass. Based on this result the limit of detection of the system described in this paper is better than 0.05 g/m² for the certified lubricant BAM K-009.

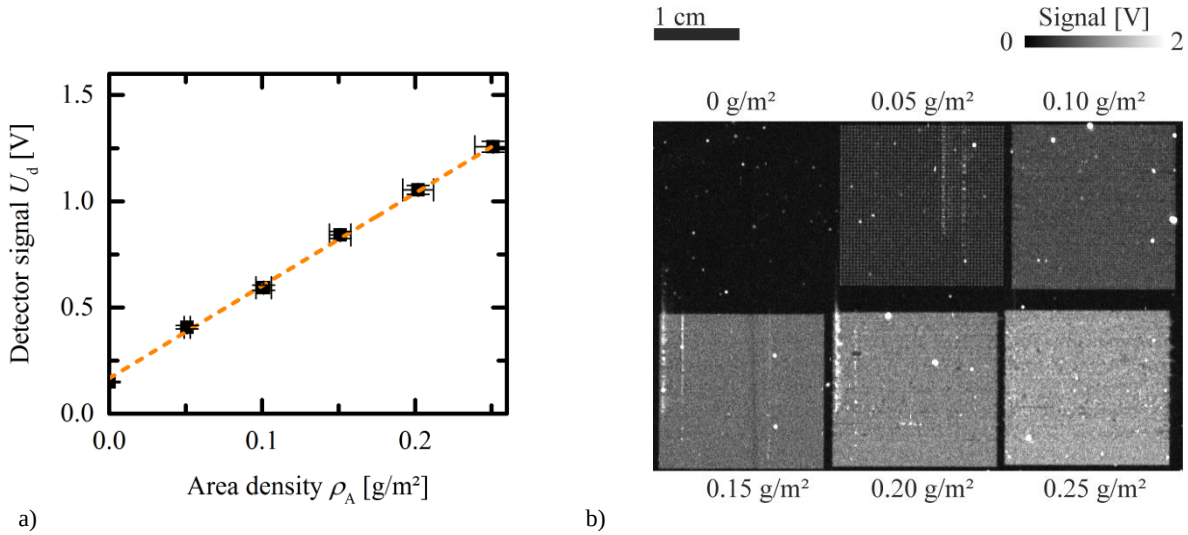

a) b)

Figure 9: Analysis of a fluorescence image (b) of a silicon wafer that was coated using an ink jet printer. The sample shown on the right (b) is coated with different area densities of the certified lubricant oil BAM K-009. Figure 9a clearly visualizes the linear relation between the fluorescence signal and the thickness of the lubricant layer.

3.5 Analysis of lubricant distribution

The main application of the presented system is the analysis of the spatial distribution of lubricants on metal surfaces. The result of the analysis of the lubricant distribution on a metal plate is shown in Figure 10a. The result of the analysis of the lubricant distribution on a freeform object is shown in Figure 10b.

The metal plate analyzed in Figure 10a was stored in a stack between other metal plates. The fluorescence image shown in Figure 10a clearly shows the possibility to visualize the inhomogeneity of the lubricant coating with the system presented in this paper. The sample analyzed in Figure 10b has approximately the size of a fist. The image shows the ability to analyze freeform objects. An accumulation of lubricant can be clearly identified in the inner edge in the upper area of the component. The depth of focus of the presented system is several centimeters due to the use of a laser beam for the fluorescence excitation.

4. CONCLUSION AND OUTLOOK

We have presented a new optical setup that is capable to monitor the spatial distribution of lubricants on metal surfaces. The setup uses scanning mirrors to deflect a laser beam on the sample surface. During the scan the excitation laser induces fluorescence locally on the probe inside the sample chamber. In this way the setup allows the acquisition of two dimensional images of lubricant distributions.

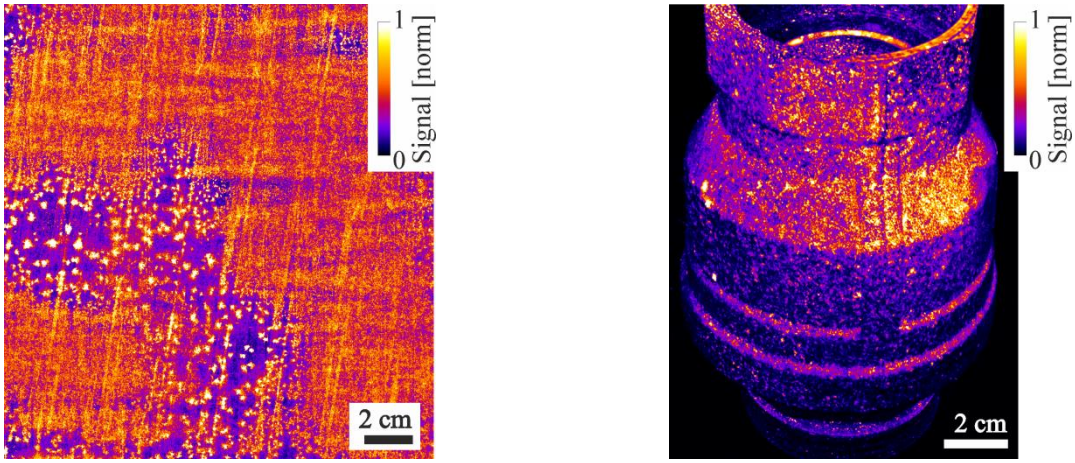

a) b)

Figure 10: Analysis of lubricant distribution on two metal surfaces acquired with system presented in this paper. The pseudo color scale is normalized to the maximum signal intensity in each image. The left image (a) clearly shows the possibility to visualize the inhomogeneity of the lubricant coatings after storing the metal plate in a stack. The right image (b) shows the ability to analyze freeform objects due to depth of focus of the presented of several centimeters.

The optical system was installed on top of a sample chamber to analyze its performance. A Repeatability better $\pm$ 2 % was determined at 5 500 measurements of a sample target made of inorganic dyes. At a height of the sample chamber of 300 mm the field of view of the presented system is 300 x 300 mm². The optical resolution of the system was analyzed using a custom made grid placed on a fluorescent target. At a scan rate of 50 lines per second a 1:2 contrast ratio at a grid period of 0.4 mm was determined. This means that gaps between lubricant droplets down to a width of 200 µm can still be visualized by the analyzed system.

For the calibration of the system samples containing well-defined lubricant layers were prepared using an ink jet printer. For this experiment the certified reference material BAM-K009 was used as lubricant. This experiment shows the linear relation between the fluorescence signal and the thickness of the lubricant layers for the prepared samples.

Thus the presented technology for the first time allows a spatial resolution in the millimetre range at production speed. The presented test system analyses an area of 300 x 300 mm² at spatial resolution of 1.1 mm in less than 20 seconds. Despite this high speed of the measurement the limit of detection of the system described in this paper is better than 0.05 g/m² for the certified lubricant BAM K-009.

The field of view of the presented system is limited by the height of the sample chamber. The scan speed of the presented system is limited by the mechanical inertia of the utilized mirrors. To overcome these limitations an enhanced scanner system using a polygon mirror is under development. This enhanced system will be tested directly in the production line.

ACKNOWLEDGMENTS

We thank Stefan Adolph and Andreas Sutorius for the CAD Design after the first breadboard setup was established. We thank Jens Scherer for many fruitful discussions about the electronics of the presented system. We thank Bastian Knabe for the great team work in the beginning of the project leading to the work, which is presented in this paper. We thank Sebastian Wolf for providing the etched aluminium stencil. We thank Kathrin Kambeck, Thanh Mai Pham and Andreas Falk for doing a lot of the measurements leading to this work.

The research leading to these results has received funding from the Fraunhofer Gesellschaft.

REFERENCES

[1] Bilstein, W., Enderle, W., Moreas, G., Oppermann, D., Routschek, T.., Van De Velde, F., "Two systems for on-line oil film and surface roughness measurement for strip steel production," Rev. Métallurgie **104**(7–8), 348–353 (2007).

[2] Schreiner, C., "EMG SOLID® IR and LIF: Two systems, one DNA," <http://www.emg-automation.com/en/details/emg-solidr-ir-und-lif-zwei-systeme-eine-dna/> (10 April 2017).

[3] Bley, H.., Oberhausen, M., "Metrological approaches for meeting the requirements of clean production," Towar. a Closed Loop Econ. 13th CIRP Int. Conf. Life Cycle Eng., 619–622 (2006).

[4] Morton, C. E., Baker, R. C.., Hutchings, I. M., "Measurement of liquid film thickness by optical fluorescence and its application to an oscillating piston positive displacement flowmeter," Meas. Sci. Technol. **22**(12), 125403 (2011).

[5] Wigger, S., Füßer, H.-J., Fuhrmann, D., Schulz, C.., Kaiser, S. A., "Quantitative two-dimensional measurement of oil-film thickness by laser-induced fluorescence in a piston-ring model experiment," Appl. Opt. **55**(2), 269 (2016).

[6] Hengstermann, T.., Reuter, R., "Laser Remote Sensing of Pollution of the Sea: a Quantitative Approach," EARSeL Adv. Remote Sens. **1**(2–II), 52–60, European Association of Remote Sensing Laboratories (1992).

[7] Hengstermann, T.., Reuter, R., "Lidar fluorosensing of mineral oil spills on the sea surface.," Appl. Opt. **29**(22), 3218–3227 (1990).

[8] Labsphere Inc., "Datasheet Spectralon Diffuse Fluorescence Materials," 2015, <http://labsphere.com/labsphere-products-solutions/materials-coatings-2/coatings-materials/fluorescence-materials/> (10 April 2017).

[9] Valeur, B., Molecular Fluorescence, Wiley-VCH Verlag GmbH, Weinheim, FRG (2001).

[10] Panne, U.., Nehls, I., "Datasheet: Certified Reference Material BAM-K009," 2006, <https://www.webshop.bam.de/product_info.php?cPath=2282_2308&products_id=8740> (10 April 2017).